Model-Based Estimation of Active and Passive Muscle Forces Using MRE in Forearm Muscles During 2-DOF Wrist Tasks

Cody Helm[1] and Fabrizio Sergi[1]

***Abstract*— Magnetic resonance elastography (MRE)-based muscle force estimation methods have been proposed to estimate individual muscle forces based on measurements of shear wave speed and joint torque in multiple postures. To estimate both the slope and offset parameters of the relationship between shear-wave speed and muscle force, it is necessary to collect measurements in a plethora of postures in case of substantial muscle redundancy. However, anisotropic MRE requires a structural and diffusion-tensor imaging scan in each posture, which is infeasible given the time constraints of MRI imaging.**

The objectives of this work were to develop a muscle force with sufficient accuracy that would only require a limited set of postures, and to evaluate its effectiveness under a variety of measurement conditions. We developed a novel MRE-based muscle force estimator, which decouples shear wave speed into its active and passive components and solves for the slope and offset parameters, independently. We assessed the effectiveness of the proposed estimator under different simulated measurement conditions, with varying levels of noise, and compared it to the original MRE-based estimator.

The proposed muscle force estimator results in a reduction in the estimation error for the offset parameter, for all muscles, without significant degradation in the estimation error for the slope parameter. However, the proposed muscle force estimator does not improve the goodness-of-fit compared to the original estimator, though cross-validation error is improved relative to the original estimator in high measurement error conditions. In conclusion, the proposed MRE-based muscle force estimator improves the estimation of muscle-specific parameters and may yield increased muscle force estimation performance.

I. INTRODUCTION

Knowledge of how the musculoskeletal systems distributes joint load amongst individual muscles is one of the grand-challenges of biomechanics. Insight of individual muscle force contributions would provide guidance into the design of human-interacting robotic systems and prostheses [1], experimental validation for musculoskeletal models [2], and an improved understanding of motor impairment diagnosis and progression in musculoskeletal injuries [3].

One method to quantify individual muscle force involves muscle activity measurements with muscle force calibration procedures. This method combines surface electromyography (sEMG) recordings from individual muscles with joint torques and a musculoskeletal model to compute estimates of individual muscle force [4], [5]. These methods have shown promise in both static and dynamic muscle contractions [6], [7]. However, in wrist tasks where non-superficial muscles contribute substantially to the resultant joint torque, sEMG-based estimates of muscle force can be significantly inaccurate due to the presence of un-measurable function from non-superficial muscles and cross-talk between adjacent muscles. Ultrasound elastography, a shear wave elastography(SWE) technique, has been developed to evaluate individual muscle function. Ultrasound elastography can quantify the mechanical properties of individual muscles [3], [8], [9], and establish the relationship between shear wave speed and skeletal muscle force undergoing static and dynamic contractions. While ultrasound elastography offers excellent temporal resolution, it is also limited in its ability to measure the shear wave speed in non-superficial muscles.

Magnetic resonance elastography(MRE) incorporates MRI imaging to measure the shear wave speeds of skeletal muscles in a 3D tissue volume. This enables to measure the muscle shear stiffness at a larger field-of-view. Shear wave speed of upper extremity muscles such as the biceps brachii [10] and the flexor digitorium profundus (FDP) have been quantified with MRE during rest and active contractions. MRE is sensitive to detect differences in muscle mechanical properties associated with injured muscles compared to healthy muscles [11]. Recently, our group has shown that MRE can be used to estimate individual muscle forces in the forearm in humans during isometric wrist contractions based on repeated measurements in different postures [12]. This work has shown that shear wave speed squared measurements can explain 70% of the variance in wrist torque via a linear regression model and can back estimate wrist torque with 30% average torque error [12].

One limitation of most previous muscle MRE work is the assumption of an isotropic material in estimating the relationship between the measured displacement field and the shear wave modulus, G. New methods for anisotropic MRE imaging have been proposed [13], [14], and they account for the mechanical properties of muscle fibers when solving the non-linear inversion algorithm and obtaining the shear stiffness 3D tissue maps. On the one hand, MRE protocols based on a larger number of postures are advantageous because they allow to differentiate the independent contribution of multiple agonist and antagonist muscles acting around the wrist joint to produce joint torque. On the other hand, however, the use of large number of postures in an MRE protocol may be non-viable experimentally due to the need of collecting anatomical and DTI in multiple postures, leading to participant fatigue. As such, identification of force estimation algorithms that are accurate in estimating muscle force from MRE data under a limited number of postures would allow to reap the benefits of anisotropic MRE protocols.

[1]Fabrizio Sergi is with the Departments of Biomedical Engineering and Mechanical Engineering, The Human Robotics Lab, University of Delaware, Newark, DE, 19713 fabs@udel.edu

Towards the goal of enabling the use of anisotropic MRE protocols for estimating individual muscle force, this paper presents the development of a new muscle force estimator that can be adequately combined with anisotropic MRE to accurately estimate the parameters of the shear-wave speed to force relationship for all thirteen forearm muscles and evaluate its effectiveness in estimating muscle force under a variety of experimental conditions.

II. Materials and Methods

A. Muscle Mechanics

Our previous work reviews the derivation of the mathematical relationship between shear wave speed measurements and muscle forces [12]. Here, we will provide a brief summary of the derivation to enable us to use this relationship in the muscle force estimator.

The outcome from MRE data are muscle-specific measurements of shear-wave speed obtained through the calculated shear stiffness, μ, and the density of skeletal muscle, ρ, ($v_{SH}^2 = \mu/\rho$). The relationship between shear-wave speed and muscle force can be described by combining the relationship between muscle force (f_{MT}) and axial load (σ), the relationship between Young's modulus (E) and shear modulus (G), and the relationship between shear wave velocity and axial load and shear modulus. Muscle force is related to the axial load in the muscle through its cross-sectional area (A_{CS}).

$$\sigma = \frac{f_{MT}}{A_{CS}} \tag{1}$$

In muscle tissue, E increases linearly with the axial stress (σ) from a starting unstressed value (E_0) with a slope of α [8].

$$E = \alpha\sigma + E_0 \tag{2}$$

It has been shown that there is a linear relationship between Young's modulus (E) and shear modulus for skeletal muscles [8]. Thus, with knowledge of a linear proportionality constant, β, we can obtain the stiffness of the muscle.

$$G = \frac{E}{\beta} \tag{3}$$

Shear-wave speed is a function of both shear modulus, G, and axial load, σ, for axially isotropic materials. Martin et al., [9] provides a relationship between shear-wave speed squared (SWSS), shear modulus, and axial load:

$$v_{SH}^2 = \frac{k'G + \sigma}{\rho} \tag{4}$$

Thereby, substituting (1), (2), and (3) into (4), we obtain a relationship between SWSS and muscle force. The resulting equation is a linear relationship between muscle force and SWSS with a slope γ and offset κ:

$$f_{MT} = v_{SH}^2\gamma - \kappa \tag{5}$$

Thus, muscle forces can be obtained from SWSS measurements once the muscle-specific parameters γ and κ have been determined.

B. Muscle Force Estimation

To determine the parameters γ and κ for the muscle-specific relationship between SWSS and muscle force, we formulated a muscle force estimation procedure that extends the one presented in previous work [15]. The muscle force estimator combines measurements of SWSS, wrist torques, and wrist postures with parameters extracted from a musculoskeletal model [16], which includes m muscles spanning the wrist joint. A muscular Jacobian matrix, $\mathbf{J}$, was obtained for each of the m muscles and considered wrist postures from the musculoskeletal model via OpenSim [15]. Components of matrix $\mathbf{J}$ are the moment arm values with each row corresponding to one of the n wrist DOFs, and each column corresponding to a specific muscle, resulting in $\mathbf{J}$ being a $n \times m$ matrix. In this work, we consider $n = 2$, as we consider torque production in the flexion/extension (FE), and radial/ulnar deviation (RUD) axes. For estimation, a $n \times 1$ wrist torque vector $\boldsymbol{\tau} = [\tau_{FE}; \tau_{RUD}]$ measured during each isometric contraction using the MREbot [15] is related to the $m \times 1$ muscle force vector as:

$$\boldsymbol{\tau} = -\mathbf{J}\mathbf{f}_{\mathbf{MT}} \tag{6}$$

By substituting the relationship between muscle force, $\mathbf{f}_{\mathbf{MT}}$, and SWSS, $\mathbf{v}_{\mathbf{SH}}^{\mathbf{2}}$, into the previous equation, we obtain the relationship between SWSS measurements and the wrist torques:

$$\boldsymbol{\tau} = -\mathbf{J}\boldsymbol{\Gamma}\mathbf{v}_{\mathbf{SH}}^{\mathbf{2}} + \mathbf{J}\boldsymbol{\kappa} \tag{7}$$

where $\mathbf{v}_{\mathbf{SH}}^{\mathbf{2}}$ is a $m \times 1$ vector that contains the measurements of SWSS for each muscle, $\boldsymbol{\Gamma} = \text{diag}(\gamma_1, \gamma_2, ..., \gamma_{13})$ is a $m \times m$ matrix that contains muscle-specific slope constants in its diagonal elements, and $\boldsymbol{\kappa}$ is a $m \times 1$ vector that contains the muscle-specific offset constants.

Overall, the equation above is a linear equation of the form $\boldsymbol{X_l\beta} - \boldsymbol{y_l} = 0$, where $\boldsymbol{X_l} = [-\boldsymbol{J}\boldsymbol{v}_{\boldsymbol{SH}}^{\boldsymbol{2}}\ \boldsymbol{J}]$ is a $n \times 2m$ matrix obtained by horizontal concatenation of a $n \times m$ matrix with elements $-\boldsymbol{J_{ij}}\ \boldsymbol{v}_{\boldsymbol{SH,j}}^{\boldsymbol{2}}$ and the $\boldsymbol{J}$ matrix; $\boldsymbol{\beta} = [\boldsymbol{\gamma}; \boldsymbol{\kappa}]$ is a $2m \times 1$ vector of unknowns obtained by vertical concatenation of the unknown parameter vectors $\boldsymbol{\gamma} = (\gamma_1, \gamma_2, ..., \gamma_m)^T$ and $\boldsymbol{\kappa} = (\kappa_1, \kappa_2, ..., \kappa_m)^T$ and $\boldsymbol{y_l} = \boldsymbol{\tau_l}$, and subscript l indicates each contraction. By collecting data during N isometric contractions at different wrist postures, it is possible to construct a $nN \times 2m$ matrix $\boldsymbol{X} = [\boldsymbol{X_1}; \boldsymbol{X_2}; ...; \boldsymbol{X_N}]$ via vertical concatenation of the contraction-specific $\boldsymbol{X_l}$ matrices to account for the nN measurements $\boldsymbol{y} = (\boldsymbol{\tau}_1, \boldsymbol{\tau}_2, ..., \boldsymbol{\tau}_l)^T$.

Using least squares regression, it is then possible to estimate the vectors $\hat{\boldsymbol{\gamma}}$ and $\hat{\boldsymbol{\kappa}}$ given measurements of joint torque, SWSS, and knowledge of the moment arm matrix $\boldsymbol{J}$ from a musculoskeletal model. After estimating $\hat{\boldsymbol{\gamma}}$ and $\hat{\boldsymbol{\kappa}}$, the estimated parameters can be used to convert measurements of SWSS to estimates of muscle force using (5).

The second term $\boldsymbol{J}$ in the matrix $\boldsymbol{X_l}$ is a $n \times m$ matrix (in general, a wide matrix: $m > n$ due to muscle redundancy) whose elements are obtained based on wrist posture. The same $\boldsymbol{J}$ is used for all contractions that occur in a single posture. Therefore, the number of linearly independent rows in this matrix is a maximum of n, or 2. For an experimental

protocol with P postures, the rank r of the experimental matrix $\mathbf{X}$, is defined as:

$$r = m + nP \tag{8}$$

The r also corresponds to the number of parameters that can be estimated. For all parameters in $\boldsymbol{\beta}$ to be estimated, $r \geq 2m$.

For the case of forearm MRE, $m = 13$ and $n = 2$, so this algorithm would require to collect data in seven wrist postures for the experimental matrix to be full-rank, i.e. $r > 2m$. For anisotropic MRE muscle imaging protocols, structural MRI images and a DTI scan are required to define muscle segments and tract the muscle fibers in each additional wrist posture. Due to the time-constraints of MRI experiments, it is not possible to collect MRE measurements in seven different wrist postures in a single session without inducing significant effects of participant fatigue, or requiring structural images to be collected in separate sessions. Therefore, there is a need to develop a muscle force estimator to allow for estimating all unknown parameters even in the presence of a limited number of wrist postures.

C. Proposed Muscle Force Estimator

The proposed muscle force estimator aims to estimate both $\hat{\boldsymbol{\gamma}}$ and $\hat{\boldsymbol{\kappa}}$ for all muscles by decoupling equation (7) into its active and passive components to solve for each parameter individually. First, the set of $\mathbf{v^2_{SH}}$ measurements is decoupled into active and passive components. The passive SWSS matrix $\mathbf{v^2_{SH_{pass}}}$ is computed for each posture as a $P \times m$ matrix, where P is the number of postures. Each row p of $\mathbf{v^2_{SH_{pass,p}}}$ is computed as the average of $\mathbf{v^2_{SH}}$ values measured over multiple repetitions k during rest for each posture p:

$$\mathbf{v^2_{SH_{pass,p}}} = \text{mean}_k(\boldsymbol{v^2_{SH_{rest,k,p}}}) \tag{9}$$

The active SWSS matrix, $\mathbf{v^2_{SH_{act}}}$, is $N \times m$, where N is the number of contractions. The rows of $\mathbf{v^2_{SH_{act}}}$ are obtained by subtracting the posture-specific $\mathbf{v^2_{SH_{pass,p}}}$ from the measured $\mathbf{v^2_{SH}}$ in that posture for all N contractions. For each posture p and contraction l,

$$\mathbf{v^2_{SH_{act,l}}} = \mathbf{v^2_{SH_{l,p}}} - \mathbf{v^2_{SH_{pass,p}}} \tag{10}$$

Wrist torques $\boldsymbol{\tau}$ are also decoupled into active and passive components. For each contraction, the passive joint torque, $\boldsymbol{\tau_{pass}}$, is a $n \times 1$ vector resulting from passive muscle forces, $\mathbf{f_{pass}}$, which are posture-specific and estimated from a musculoskeletal model [16].

$$\boldsymbol{\tau_{pass,p}} = -\mathbf{J}\mathbf{f_{pass,p}} \tag{11}$$

During MRE data collections, at each new posture the force/torque sensor is zeroed with the participant at rest to remove any non-zero torque values resulting from the contribution of passive muscle force in that posture [12]. Thus, the active torque, $\boldsymbol{\tau_{act}}$, is a $n \times 1$ vector equal to the measured torque values, $\boldsymbol{\tau_m}$. Parameter estimation is performed using first the active torque values for all N contractions to obtain the muscle specific $\hat{\boldsymbol{\gamma}}$ slopes, i.e., by solving the equation below for $\boldsymbol{\Gamma}$ using ordinary least squares regression.

$$\boldsymbol{\tau_{act}} = -\mathbf{J}\boldsymbol{\Gamma}\mathbf{v^2_{SH_{act}}} \tag{12}$$

The experimental matrix for this design is a tall matrix with dimensions $(nN) \times m$, with linearly independent columns, and thus an m-rank matrix. As such, it is possible to solve for the muscle-specific slope coefficients for each of the m muscles using ordinary least squares.

Once the muscle-specific slope coefficients are determined as $\hat{\boldsymbol{\gamma}}$, and $\hat{\boldsymbol{\Gamma}} = diag(\hat{\gamma}_1, \hat{\gamma}_2, ..., \hat{\gamma}_m)$, $\boldsymbol{v^2_{SH_{pass,p}}}$ and $\boldsymbol{f_{pass,p}}$ are used to obtain the $\hat{\boldsymbol{\kappa}}$ coefficients for all muscles and each posture p.

$$\boldsymbol{\tau_{pass,p}} = -\mathbf{J}\hat{\boldsymbol{\Gamma}}\boldsymbol{v^2_{SH_{pass,p}}} + \mathbf{J}\boldsymbol{\kappa_p} \tag{13}$$

From here, we can substitute (11) in the expression for torque, and then simplify $\mathbf{J}$ from the equation, solving for the unknown set of parameters $\hat{\boldsymbol{\kappa}}$.

$$\boldsymbol{\kappa_p} = \hat{\boldsymbol{\Gamma}}\mathbf{v^2_{SH_{pass,p}}} - \mathbf{f_{pass,p}} \tag{14}$$

The muscle-specific $\hat{\boldsymbol{\kappa}}$ offset terms are determined by taking the average over all wrist postures.

$$\hat{\boldsymbol{\kappa}} = \text{mean}_p(\boldsymbol{\kappa_p}) \tag{15}$$

D. Model-Based Simulations of Shear Wave Speed Squared Measurements

We simulated virtual experiments where the quantities of $\boldsymbol{v^2_{SH,m}}$ and $\boldsymbol{\tau_m}$ were measured for a given experimental protocol composed of N isometric contractions to investigate the accuracy of our proposed estimator compared to the original estimator. Each contraction was defined as an isometric wrist torque applied at a specific wrist posture. For each contraction, we obtained simulated values of muscle forces using an optimization based, redundancy solver that aimed to minimize the global activation level ($GAL = \sum_j (activations_j)^2$) with the $\boldsymbol{J}$ and $\boldsymbol{\tau_m}$. With known values of $\hat{\boldsymbol{\gamma}}$ and $\hat{\boldsymbol{\kappa}}$, simulated muscle forces were converted to simulated SWSS values. Then, we introduced various forms of physiological variability and measurement noise into the simulated SWSS values to test the effectiveness of each estimator under different experimental noise and variance. The final simulated $\boldsymbol{v^2_{SH}}$ matrix was included with the desired wrist torque values and $\boldsymbol{J}$ in an ordinary least-squares regression to obtain muscle-specific estimates of $\hat{\boldsymbol{\gamma}}$ and $\hat{\boldsymbol{\kappa}}$.

E. Evaluation of Estimators

We conducted virtual experiments where measurements of $\boldsymbol{v^2_{SH}}$ were simulated under different noise levels and experimental protocols defined as a set of wrist torques and wrist postures. Similarly to our previous work [15], we applied two forms of noise/variance into the simulated SWSS values: 1) Physiological variability, ϵ^A, was implemented to account for non-optimal muscle contraction patterns that can be used to achieve the desired wrist torque; 2) Measurement noise, ϵ^M, was implemented to account for variance in data quality. For each noise level, the amount of noise incorporated

into the simulated SWSS measurements was taken from a continuous uniform distribution. For each virtual experiment, ϵ^M and ϵ^A were selected from uniform distributions with $\epsilon_{max} \in$ [0 0.5 1]. The distribution for $\epsilon^A = [0, \epsilon^A_{max}]$ and $\epsilon^M = [-\epsilon^M_{max}, \epsilon^M_{max}]$. For each noise level, we simulated N=50 virtual experiments. We considered two models, the original muscle force estimator and the proposed muscle force estimator. We considered the finger muscles to be active and contribute in generating the measured wrist torque. For all virtual experiments, we included the measurements from all forearm muscles to reproduce conditions of MRE imaging.

We considered three different experimental protocols defined based on wrist postures and repetitions. We simulated virtual experiments for a five posture / one repetition (5P/1R), a two posture / one repetition (2P/1R), and a two posture / three repetition (2P/3R) protocol. The wrist postures for the five posture protocol were defined as $([\theta_{FE}, \theta_{RUD}] \in [-30, 0], [-15, 0], [0, 0], [15, 0], [30, 0]^\circ)$ and the the wrists for the two posture protocol were defined as $[-15, 0], [15, 0]^\circ$. For all protocols, the desired wrist torques were defined as unitary magnitude in all four cardinal directions, flexion, extension, radial deviation and ulnar deviation, as well as a rest condition. For all contractions, we simulated $\boldsymbol{v^2_{SH}}$ measurements with γ = 10 and κ = 500 for all muscles.

For the muscle level analysis, we obtained estimates of $\hat{\boldsymbol{\gamma}}$ and $\hat{\boldsymbol{\kappa}}$ using both the original and proposed estimator in all experimental protocols and noise combinations. We quantified the accuracy of each estimator by computing the percent error in estimating $\hat{\boldsymbol{\gamma}}$ and $\hat{\boldsymbol{\kappa}}$ for all m forearm muscles. $\hat{\boldsymbol{\gamma}}$ and $\hat{\boldsymbol{\kappa}}$ error for the five main wrist muscles (ECRL, ECRB, ECU, FCR, and FCU) were computed by taking the median percent error over those muscles. $\hat{\boldsymbol{\gamma}}$ and $\hat{\boldsymbol{\kappa}}$ error for all muscles were obtained by taking the median percent error across those muscles.

Under the model assumptions, the force measured from multiple muscles spanning the wrist joint should sum as described in (6) to yield the measured value of joint torque accounting for passive joint torque. In other words, if $\hat{\boldsymbol{\gamma}}$ and $\hat{\boldsymbol{\kappa}}$ are the estimated muscle-specific parameters and $\boldsymbol{\Gamma} = diag(\hat{\gamma})$, the joint torques resulting from the estimated muscle forces $\boldsymbol{\tau_{est}} = -\boldsymbol{J\Gamma v^2_{SH}} + \boldsymbol{J\kappa}$ should be equal to joint torque values $\boldsymbol{\tau_m}$ measured via the F/T sensor along with the passive wrist torques.

To quantify how well the estimators were able to reconstruct the joint-level torque, we obtained R^2 goodness of fit values for each virtual experiment and estimator type. For both estimators, the R^2 value was obtained by comparing the back-estimated torques predicted by each estimator, from eq. (7), and the desired torques.

Moreover, since the estimators use a different set of parameters, and are thus not directly comparable based on R^2, we also performed a leave-one-out cross validation (LOOCV) analysis. We quantified the LOOCV error as the unsigned difference between the estimated torque value of the unseen wrist contraction and the desired wrist torque for that contraction. For each virtual experiment, we computed the average LOOCV error as the average over all N contractions. Then, as a proxy to quantify the accuracy of muscle force estimation, we quantified the torque estimation bias $\boldsymbol{b_\tau}$, separately, for each contraction,

$$\boldsymbol{b_\tau} = \boldsymbol{\tau_{est}} - \boldsymbol{\tau_m} \tag{16}$$

III. Results

Muscle and joint level analysis results for the original and proposed muscle force estimators for all experimental conditions are shown below.

A. Muscle Level Analysis

For the wrist muscles, in the highest noise level, the original estimator yields 0.23, 0.40, and 0.21 $\hat{\gamma}$ error for the 5P/1R, 2P/1R, and 2P/3R protocols, respectively, while the proposed estimator yields 0.23, 0.43, and 0.25 $\hat{\gamma}$ error, respectively. For both estimators, $\hat{\gamma}$ error for wrist muscles increases with ϵ^M but not ϵ^A. Additionally, $\hat{\gamma}$ error decreases with an increase in postures and repetitions.

For the wrist muscles, for the highest noise level, the original estimator yields 2.16, 0.91, and 0.86 $\hat{\kappa}$ error for the 5P/1R, 2P/1R, and 2P/3R protocols, respectively, while the proposed estimator yields 0.04, 0.08, and 0.04 $\hat{\kappa}$ error, respectively. $\hat{\kappa}$ error increases with ϵ^M but not ϵ^A for both estimators. The 2 posture protocols result in similar $\hat{\kappa}$ error, while the 5 posture protocol results in a larger $\hat{\kappa}$ in the original estimator in high measurement noise.

B. Joint Level Analysis

For the highest noise level, the original estimator yields an R^2 of 0.88, 0.94, and 0.84 for the 5P/1R, 2P/1R, and 2P/3R, respectively. The proposed estimator yields an R^2 of 0.79, 0.86, and 0.81 for the 5P/1R, 2P/1R, and 2P/3R, respectively. R^2 decreases with an increase in ϵ^M for both estimators but does not vary with ϵ^A for either estimator. R^2 increases with less repetitions per contraction and decreases for more postures. Statistical analysis showed that the original estimator

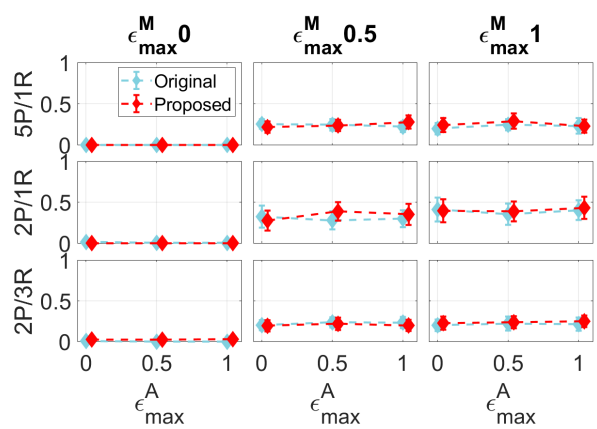

Fig. 1. Median $\hat{\gamma}$ error [n.u.] for wrist muscles grouped by noise condition (columns), protocol (rows), physiological noise (x axis), and estimator (overlay). Diamonds indicate the between-runs median and the whiskers extend to $\pm$ 1 standard deviation.

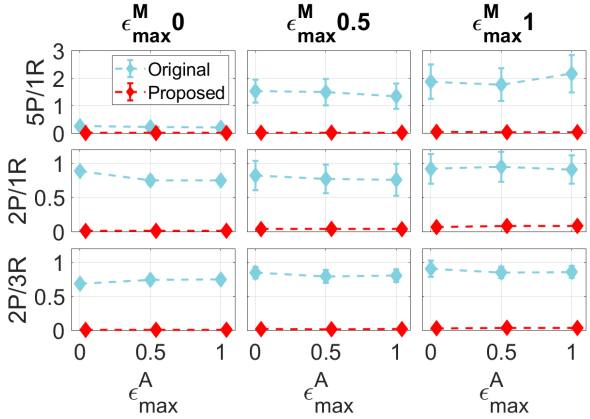

Fig. 2. Median $\hat{\kappa}$ error [n.u.] for wrist muscles grouped by noise condition, protocol, physiological noise, and estimator. Diamonds indicate the between-runs median and the whiskers extend to $\pm$ 1 standard deviation.

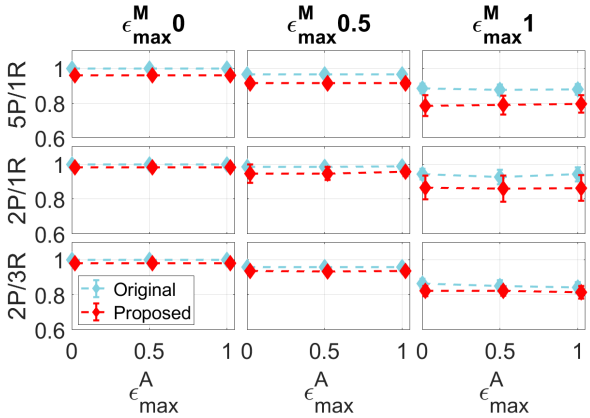

Fig. 3. Mean goodness of fit (R^2) values grouped by noise condition, protocol, physiological noise, and estimator. Diamonds indicate the between-runs mean and the whiskers extend to $\pm$ 1 standard deviation.

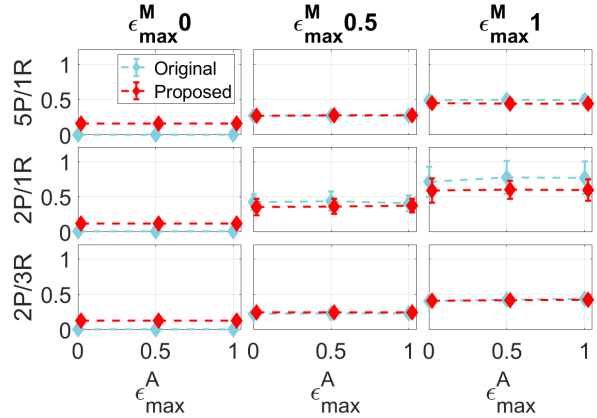

Fig. 4. Mean LOOCV error [Nm] values grouped by noise condition, protocol, physiological noise, and estimator. Diamonds indicate the between-runs mean and the whiskers extend to $\pm$ 1 standard deviation.

yielded a significantly higher R^2 value than the proposed for high noise levels.

For the highest noise level, the original estimator yields an average LOOCV error of 0.50, 0.77, and 0.43 Nm for the 5P/1R, 2P/1R, and 2P/3R, respectively, while the proposed estimator yields an average LOOCV error of 0.44, 0.59, and 0.42 Nm, respectively. Paired comparisons indicate that LOOCV error of the proposed estimator is significantly smaller than the original estimator (t=6.33,p <0.001) for $\epsilon^M_{max} = 1.0$ conditions, including data from all protocols. When considering the 5P/1R protocol, the proposed estimator is still significantly better in terms of LOOCV (t=6.97,p <0.001), but that is not the case for the 2P/3R protocol (t=0.57,$p = 0.28$). LOOCV error increases with ϵ^M but does not vary with ϵ^A for both estimators. LOOCV error decreases with an increase of postures and repetitions.

For a high noise level, the proposed estimator yields a higher back-estimated torque variation compared to the original estimator for all protocols. FE $\boldsymbol{b_\tau}$ is slightly higher in the proposed estimator than the original in the 5P/1R and 2P/1R protocols, while the RUD $\boldsymbol{b_\tau}$ is slightly higher in the proposed than original estimator in the 5P/1R and 2P/3R protocols.

IV. Discussion

The work in this paper presents a novel muscle force estimator for MRE-based measurements that decouples the measured torques and shear-wave speeds (SWS) to estimate the slope and offset coefficients for the linear relationship between SWS squared and muscle force. Ordinary least squares regression is performed with the measured active SWS to obtain the slope coefficients for all muscles. Then, the estimated slope coefficients are combined with the measured passive SWS and model-estimated forces to obtain the offset coefficients. We hypothesized that the proposed estimator would improve the accuracy of the muscle force estimation compared to the original estimator. To test this hypothesis, we quantified the estimated parameter error for all muscles for both estimators. Additionally, we computed the average goodness of fit R^2 value, average LOOCV error, and the back-estimated torque bias to evaluate the accuracy of each estimator using analyses that can be replicated

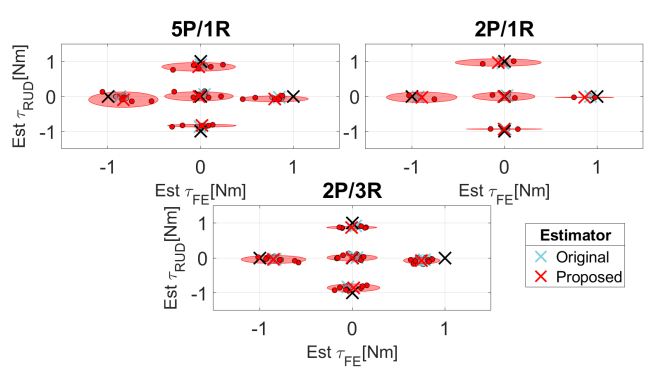

Fig. 5. Back-estimated wrist torque mean and 95% confidence intervals plotted for each estimator (overlay) for a high noise level, and protocol (subplots). Black crosses indicate the cued torque value. Each dot represents the between-run average of the back-estimated torque corresponding to a given contraction state.

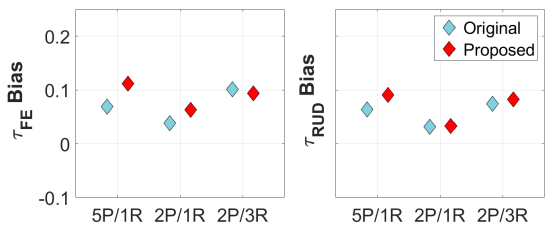

Fig. 6. Average torque bias ($\boldsymbol{b_\tau}$) [Nm] for each experimental protocol (x axis) and estimator (colors), for a high noise level.

experimentally.

Overall, the muscle level analysis shows that the proposed estimator decreases the $\hat{\kappa}$ estimation error compared to the original estimator for all protocols and noise levels with comparable $\hat{\gamma}$ error between both estimators. $\hat{\gamma}$ and κ error increase with ϵ^M but not ϵ^A. For joint level analysis, the proposed estimator yield a lower average LOOCV error for high noise combinations, while the original estimator results in a higher R^2. Both R^2 and LOOCV error worsen with an increase in ϵ^M but not ϵ^A. The proposed estimator results in an increase in $\boldsymbol{b_\tau}$ and back-estimated torque variability compared to the original estimator. Taken together, the proposed muscle force estimator improves the overall parameter estimation accuracy, but reduces the back-estimated torque accuracy compared to the original estimator.

The proposed estimator greatly reduces $\hat{\kappa}$ estimation error with a comparable $\hat{\gamma}$ error for both estimators. As $\hat{\gamma}$ is torque dependent, the capability of estimating $\hat{\gamma}$ is not expected to change with decoupling the experimental matrix. With the proposed estimator, $\hat{\kappa}$ is estimated for all muscles resulting in a lower estimation error. Previous studies have shown accuracy in using rest contractions to estimate the passive muscle force components [12], [17]. The original estimator yields a higher R^2 value than the proposed estimator. One explanation for this is that the original estimator encompasses more parameters when solving the least-squares regression model and therefore can better fit the data to the wrist torques. This is beneficial for R^2 but in cases of high measurement noise can lead to high parameter estimation error. The proposed estimator yields a significantly lower LOOCV in several measurement and protocol conditions, suggesting that it generalizes well to an independent data set.

Back-estimated torque analysis shows that the proposed estimator results in an increase in torque bias and variability compared to the original estimator in a high noise level. The proposed estimator yields slightly higher FE $\boldsymbol{b_\tau}$ compared to the original estimator. One explanation might be that in the proposed estimator $\hat{\kappa}$ is obtained for each muscle without minimizing the estimated torque residuals. Thus, for high noise levels, the estimated torque may be more biased. For high noise combinations, the 2P/3R protocol is advantageous in minimizing parameter estimation error and LOOCV error. The proposed estimator offers an improvement in estimating the offset coefficient which can be applied to better quantify passive muscle forces.

References

[1] E. Scheme and K. Englehart, "Electromyogram pattern recognition for control of powered upper-limb prostheses: State of the art and challenges for clinical use," *Journal of Rehabilitation Research and Development*, vol. 48, no. 6, pp. 643–660, 2011.

[2] Y. K. Tamilselvam, J. Ganguly, R. V. Patel, and M. Jog, "Musculoskeletal model to predict muscle activity during upper limb movement," *IEEE Access*, vol. 9, pp. 111472–111485, 2021.

[3] F. Hug, K. Tucker, J. L. Gennisson, M. Tanter, and A. Nordez, "Elastography for Muscle Biomechanics: Toward the Estimation of Individual Muscle Force," *Exercise and Sport Sciences Reviews*, vol. 43, no. 3, pp. 125–133, 2015.

[4] C. Castellini, P. Van Der Smagt, G. Sandini, and G. Hirzinger, "Surface EMG for force control of mechanical hands," *Proceedings - IEEE International Conference on Robotics and Automation*, pp. 725–730, 2008.

[5] D. Staudenmann, K. Roeleveld, D. F. Stegeman, and J. H. van Dieen, "Methodological aspects of SEMG recordings for force estimation - A tutorial and review," *Journal of Electromyography and Kinesiology*, vol. 20, no. 3, pp. 375–387, 2010.

[6] B. Laursen, B. R. Jensen, G. Németh, and G. Sjøgaard, "A model predicting individual shoulder muscle forces based on relationship between electromyographic and 3D external forces in static position," *Journal of Biomechanics*, vol. 31, no. 8, pp. 731–739, 1998.

[7] U. Trinler, H. Schwameder, R. Baker, and N. Alexander, "Muscle force estimation in clinical gait analysis using AnyBody and OpenSim," *Journal of Biomechanics*, vol. 86, pp. 55–63, 2019.

[8] S. F. Eby, "Validation of shear wave elastography in skeletal muscle," *Journal of biomechanics*, 2013.

[9] J. A. Martin, S. C. Brandon, E. M. Keuler, J. R. Hermus, A. C. Ehlers, D. J. Segalman, M. S. Allen, and D. G. Thelen, "Gauging force by tapping tendons," *Nature Communications*, vol. 9, no. 1, pp. 2–10, 2018.

[10] M. A. Dresner, G. H. Rose, P. J. Rossman, R. Muthupillai, A. Manduca, and R. L. Ehman, "Magnetic Resonance Elastography of Skeletal Muscle," *Journal of Magnetic Resonance Imaging*, vol. 13, no. 2, pp. 269–276, 2001.

[11] S. I. Ringleb, S. F. Bensamoun, Q. Chen, A. Manduca, K. N. An, and R. L. Ehman, "Applications of magnetic resonance elastography to healthy and pathologic skeletal muscle," *Journal of Magnetic Resonance Imaging*, vol. 25, no. 2, pp. 301–309, 2007.

[12] D. R. Smith, C. A. Helm, A. Zonnino, M. D. McGarry, C. L. Johnson, and F. Sergi, "Individual Muscle Force Estimation in the Human Forearm Using Multi-Muscle MR Elastography (MM-MRE)," *IEEE Transactions on Biomedical Engineering*, vol. 70, no. 11, pp. 3206–3215, 2023.

[13] M. McGarry, E. V. Houten, C. Guertler, R. Okamoto, D. Smith, D. Sowinski, C. Johnson, P. Bayly, J. Weaver, and K. Paulsen, "A heterogenous, time harmonic, nearly incompressible transverse isotropic finite element brain simulation platform for MR elastography," *Physics in Medicine and Biology*, vol. 66, no. 5, 2021.

[14] Z. Yin, S. P. Kearney, R. L. Magin, and D. Klatt, "Concurrent 3D acquisition of diffusion tensor imaging and magnetic resonance elastography displacement data (DTI-MRE): Theory and in vivo application," *Magnetic Resonance in Medicine*, vol. 77, no. 1, pp. 273–284, 2017.

[15] A. Zonnino and F. Sergi, "Model-Based Estimation of Individual Muscle Force Based on Measurements of Muscle Activity in Forearm Muscles during Isometric Tasks," *IEEE Transactions on Biomedical Engineering*, vol. 67, no. 1, pp. 134–145, 2020.

[16] K. R. Saul, X. Hu, C. M. Goehler, M. E. Vidt, M. Daly, A. Velisar, and W. M. Murray, "Benchmarking of dynamic simulation predictions in two software platforms using an upper limb musculoskeletal model," *Computer Methods in Biomechanics and Biomedical Engineering*, vol. 18, pp. 1445–1458, 2015.

[17] G. A. Grinspan, L. Fernandes de Oliveira, M. C. Brandao, A. Pomi, and N. Benech, "Load sharing between synergistic muscles characterized by a ligand-binding approach and elastography," *Scientific Reports*, vol. 13, p. 18267, 2023.